A Low-Overhead Dynamic Formation Method for LEO Satellite Swarm Using Imperfect CSI

Chia-Hung Lin , Member, IEEE, Shih-Chun Lin , Member, IEEE, and Liang C. Chu

Abstract—In 6G systems, non-terrestrial networks (NTNs) are poised to address the limitations of terrestrial systems, particularly in unserved or underserved areas, by providing infrastructure with mobility that enhances reliability, availability, and responsiveness. Among various types of mobile infrastructures, low earth orbit (LEO) satellite communication (SATCOM) has the potential to offer extended coverage that supports numerous devices simultaneously with low latency. Consequently, LEO SATCOM attracts significant attention from academia, government, and industry. The dynamic formation problem must be solved to form a swarm connecting to the ground station with the most appropriate satellites to achieve LEO SATCOM systems with higher throughput. Existing solutions use computationally demanding methods to solve the NP-hard problem and cannot be employed for SATCOM systems with short coherence time. Furthermore, precise channel state information (CSI) between the ground station and all candidate satellites is required for formation designs, resulting in significant signaling overheads. To overcome these drawbacks, we propose a learning-based dynamic formation method for real-time dynamic formation capability. Specifically, motivated by the channel features of LEO SATCOM, we develop a CSI estimation method to provide coarse CSI (i.e., imperfect CSI) solely based on available geometrical information of LEO SATCOM and without any signaling overhead. Then, our approach can utilize the obtained coarse CSI as inputs and provide valuable guidelines as priorities to access specific satellites for fine-grained CSI (i.e., precise CSI). The prediction results are validated using a small-scale brute force method to determine the final formation. Our intensive simulation results suggest that the proposed method can aid current LEO SATCOM by providing real-time formation results, particularly in low-transmit power regions. Specifically, the proposed method can achieve 90% of full capacity with only 32% signaling overhead to build high-throughput LEO SATCOM.

Index Terms—Deep learning, dynamic formation, imperfect channel state information (CSI), low Earth orbit (LEO) satellites, multi-input multi-output (MIMO), satellite communications (SATCOM).

Manuscript received 31 October 2023; accepted 8 December 2023. Date of publication 25 December 2023; date of current version 16 May 2024. This work was supported in part by LMSSC, in part by the NC Space Grant, in part by the NC State 2022 Faculty Research and Professional Development Program (FRPD), in part by the National Science Foundation under Grant CNS-221034, in part by Meta 2022 AI4AI Research, and in part by Cisco Systems. The review of this article was coordinated by Dr. Tomaso De Cola. (Corresponding author: Chia-Hung Lin.)

Chia-Hung Lin and Shih-Chun Lin are with the Department of Electrical and Computer Engineering, North Carolina State University, Raleigh, NC 27606 USA (e-mail: clin25@ncsu.edu; slin23@ncsu.edu).

Liang C. Chu is with the Lockheed Martin Space Systems Company, Sunnyvale, CA 94089 USA (e-mail: liang.c.chu@lmco.com).

Digital Object Identifier 10.1109/TVT.2023.3347077

I. INTRODUCTION

O ENABLE novel information and communication technologies, the development of next-generation communication systems (i.e., 6G) is in full swing recently [1], [2], [3], [4], [5]. Specifically, 6G systems aim to satisfy the ever-increasing demand for the exponential growth of smart devices. Moreover, 6G systems also wish to provide the desired Quality of Service (QoS) to the above users anytime and anywhere to fully eliminate coverage blind spots. By doing so, a reliable communication system can be offered as a strong backbone to support the deployment of novel applications, such as super-smart society, connected robotics, and autonomous systems [6]. To achieve this ambitious goal, non-terrestrial networks (NTNs) are expected to provide cost-effective and high-capacity connectivity promises to complement current terrestrial networks in 6G systems. Compared to traditionally fixed infrastructure, NTNs bring infrastructure with mobility to aid the shortcomings of terrestrial systems, especially in unserved (i.g., regions under wars or severe disasters) or underserved regions (i.g., rural areas) [6], [7], [8], [9], [10]. for improved reliability, availability, and responsiveness. In light of this direction, unmanned aerial vehicle (UAV) [11], [12], [13] and satellite-enabled wireless communications [14], [15], [16], [17], [18], [19], supported by Low Earth Orbit (LEO), Medium Earth Orbit (MEO), and Geostationary Equatorial Orbit (GEO) satellites, become research hotspots in recent years.

When compared to UAV-enabled communications and their MEO/GEO counterparts, LEO satellite communication (SAT-COM) has the potential to provide extended coverage to support numerous devices simultaneously and seamlessly with low latency. Besides academia [14], [15], [16], [17], [18], [19], [20], [21], [22], [23], [24], [25], [26], this unique capability also attracts the attention of government and industry recently. For example, the United States Department of Defense is funding a project to enable seamless communication between military/government and commercial/civil satellite constellations, which currently cannot communicate with each other. Similarly, the European Union is also launching a project to build independent LEO satellite broadband communication systems. Leading companies in the SATCOM industry have also shown significant interest in LEO SATCOM. Oneweb has already launched more than 500 LEO satellites, while more than 3000 LEO satellites were operated by SpaceX. Furthermore, SpaceX plans to launch 9,000 more LEO satellites for its Starlink internet broadband constellation project, following permission from the United

0018-9545 © 2023 IEEE. Personal use is permitted, but republication/redistribution requires IEEE permission. See https://www.ieee.org/publications/rights/index.html for more information.

States Federal Communications Commission (FCC). To sum up, LEO SATCOM will undoubtedly play an important and unique role in future 6G systems.

Although LEO SATCOM offers an exciting prospect for the realization of 6G systems, the unique features and requirements of such systems also demand a re-design of communication systems. Firstly, while multi-input multi-output (MIMO) systems have proven to enhance performance in modern mobile communications, the strong line of sight (LoS) properties of LEO satellite channels require the use of a satellite swarm with multiple satellites to provide spatial diversity for MIMO. This presents new challenges that need to be addressed. Secondly, acquiring precise channel state information (CSI) is even more costly in LEO SATCOM due to the ultra-fast mobility of LEO satellites [15], [16]. This requires a significant amount of signaling overhead for CSI training (i.e., sending known pilots [27], [28]) and feedback [29], [30], [31]. Furthermore, the fast-changing CSI requires frequent CSI training and feedback, making signaling overheads an important factor to consider when designing LEO SATCOM.

In order to facilitate high throughput connectivity in LEO satellite swarm-enabled distributed MIMO communications, it is essential to address the dynamic formation problem. Specifically, given a group of candidate satellites operating in the LEO, the goal is to select a subgroup of satellites, forming a satellite swarm with the most appropriate satellites to connect to the ground station for maximized capacity. In the literature, while there are optimization-based solutions that can be applied to solve this NP-hard problem, there are two drawbacks to using them in LEO SATCOM scenarios. Firstly, existing optimization-based solutions either provide sub-optimal results or cannot provide real-time solutions, thus making it challenging to achieve a desirable trade-off between computational complexity and performance. Secondly and more importantly, acquiring precise CSI of all candidate satellites is still required for existing optimization-based solutions, which implies a significant amount of signaling overheads and is not practical for ultra-fast LEO satellites with lower coherence times. As an alternative, this work provides a practical dynamic formation solution powered by learning-based achievements to address these issues. To further elaborate, learning-based communication designs have been adopted in different mobile communications operations to address the shortcomings of traditional optimization-based methods, including [32], [33], [34], [35], [36]. Generally speaking, one motivation to introduce learning-based communication designs is to overcome the model deficit, as discussed in [37], [38], [39]. By doing so, the trained neural network can still make useful decisions even when only imperfect observation is provided as the model input. Another motivation to utilize learning-based communication designs is to solve the algorithm deficit by offloading computationally demanding operations to the offline training phase, as demonstrated in [40], [41], [42], [43]. By doing so, real-time communication operations can be used and a better trade-off can be struck in addressing the considered problem. Following this logic, we introduce learning-based communication designs to the considered problem, enabling the proposed method to work with imperfect CSI and deliver real-time capabilities to fulfill the needs of LEO SATCOM.

To do so, in the proposed method, utilizing the understanding of LEO SATCOM channels, we develop a CSI estimation method to provide coarse CSI (i.e., imperfect CSI) solely based on available geometrical information of LEO SATCOM and without any signaling overheads. Then, using the obtained coarse CSI as inputs, our approach provides valuable guidelines as priorities to access specific satellites for fine-grained CSI (i.e., precise CSI). Finally, the recommended formation results can be further validated using a small-scale brute force searching method to determine the final formation. A hyper-parameter is provided to let system designers adjust the searching range according to affordable signaling overheads and computational complexity. Our intensive simulations demonstrate that the proposed method can improve current LEO SATCOM by providing real-time formation results with low signaling overheads, particularly in regions with low transmit power. Specifically, by utilizing the developed geometrical CSI estimation, our proposed formation method can achieve at least 90% of full capacity with only 32% signaling overhead, enabling high-throughput LEO SATCOM in practice. We further validate the generalization capability of our proposed method by working with other channel estimation methods to generate coarse CSI. This approach also resulted in 90% of full capacity when the pilot-and-noise ratio (PNR) is only -20 dB, demonstrating the benefits of our proposed solution in scenarios with limited signaling overheads.

We list our contributions below:

- We develop a realistic simulation platform that investigates LEO satellite swarm-enabled distributed MIMO communications by studying the geometrical relationship between the ground station and LEO satellites. Based on the platform, we consider dynamic formation problems for LEO satellite swarms with random topology. This work represents the first attempt to determine the capacity upper bound of subsequent communication system designs in this context.
- To aid current LEO satellite swarm-enabled distributed MIMO communications, we propose a learning-based dynamic formation method to solve the aforementioned optimization problem, enabling real-time dynamic formation capability. Moreover, only a subset of precise CSI is needed, yielding significantly reduced signaling overhead when performing formation in LEO SATCOM scenarios.
- Our intensive simulation results examine the achieved performance and underlying overhead of the proposed method with different numbers of candidating satellites and different precision levels of imperfect CSI, demonstrating the effectiveness and practicality of the proposed method, particularly in regions with low transmit power and limited signaling overhead scenarios.

The rest of the paper is organized as follows. Section II discusses the related works. Section III presents the system model. Section IV formulates the dynamic LEO satellite formation problem and introduces the considered imperfect CSI models. Section V presents the proposed learning solutions. Section VI

highlights the performances of the proposed mechanism and discusses the obtained results. Finally, Section VII concludes the paper.

II. RELATED WORKS

This work aims to investigate learning-based LEO SATCOM designs, and in this section, related works in both optimizationbased and learning-based LEO SATCOM designs are reviewed. In recent developments of optimization-based LEO SATCOM designs, [14] investigates precoding design problems to maximize the ergodic sum rate in a scenario where one LEO satellite is operating in the sky to serve several ground users. With a similar scenario, [15] proposes a space angle-based user grouping algorithm to schedule served users into different groups, allowing full-frequency reuse while maximizing the achievable rate. Also focusing on applying multiple access techniques to LEO SATCOM designs, [20] develops multicast communication with rate-splitting multiple access, enabling LEO satellites to serve a group of users using the same frequency band simultaneously. By introducing a security viewpoint, [21] and [22] purpose beamforming design solutions to maximize secrecy energy efficiency and instantaneous rate, respectively, to improve the quality of service of LEO SATCOM. To further increase the practicality of the previous designs, [23] investigates the robust beamforming designs under imperfect angles of departure assumptions, and develops low complexity algorithms to fulfill the hybrid beamforming designs for LEO SATCOM. Compared with the above works concentrating on single satellite transceiver designs, this work considers an advanced scenario, where a group of LEO satellites forms a swarm and connects to a ground station (i.e., LEO satellite swarm-enabled distributed MIMO communications) for the following reason. To explain, in the industry field, several projects of new-generation large-scale LEO constellations, represented by Iridium II, Starlink, OneWeb, Telesat, and Kuiper, are operating numerous LEO satellites in the sky. By connecting those satellites as a swarm, superior connectivity can be provided by utilizing the swarm-enabled spatial diversity. Thus, there is an urgent need to investigate LEO transceiver designs in such a scenario and the developed method can be directly applied to current LEO SATCOM scenarios. Moreover, the above existing works can also be further extended to the swarm version to release the full potential of current LEO SATCOM. In light of this direction, [16] examines the relationship between inter-satellite distance in the considered swarm and the achieved capacity to provide a guideline for swarm formation. However, this work only considers an ideal case where all satellites are equally spaced in the orbit to obtain the formation conclusion. Additionally, some practical imperfections such as CSI are not discussed, limiting the direct usage to practical scenarios.

On the other hand, with these pioneering works to develop learning-based mobile communication operations in [37], [38], [40], [41], [42], researchers have investigated learning-based LEO SATCOM designs recently. For example, [17] models an interesting problem, utilizing the LEO satellite to act as

a relay for offloading the Internet of Remote Things (IoRT). A reinforcement learning-based agent is placed in the LEO satellite to decide whether to collect new IoRT data and the transmission power to relay the previously received IoRT data. Similarly, [18] also employs a reinforcement learning-based agent to configure a space link from the LEO satellite to a ground terminal for improved QoS. Furthermore, [19] investigates the usage of learning-based algorithms to aid interference detection, flexible payload configuration, and congestion prediction problems in SATCOM operations. While the proposed learningbased approaches can effectively and efficiently solve the considered multi-dimensional problems, unique features of LEO satellite swarm-enabled distributed MIMO communications are not modeled and considered in these works. Moreover, practical considerations, such as CSI imperfection and CSI training and feedback overheads, are also ignored. Finally, several studies have introduced learning-based methods for CSI prediction in LEO SATCOM scenario [24], [25], [26]. While our work and these previous studies all address CSI-related challenges in LEO satellite transceiver designs, there are two fundamental differences that distinguish our approach from theirs. Firstly, from a system modeling perspective, prior works have primarily employed conventional Rician fading channel models to simulate LEO channels. However, these models fail to adequately capture the unique characteristics of LEO satellite channels. In contrast, our approach utilizes a geometry-based LEO satellite channel model with several unique LEO factors. Hence, this model considers the distance between the satellite and the ground station and other critical LEO channel phenomena, such as atmospheric gas absorption and tropospheric scintillation. By incorporating these elements, our model provides a more realistic and practical representation of LEO satellite channels in our work. Secondly, it's worth noting that previous works only focus on predicting future CSI based on historical perfect CSI using time-series analysis. This approach implies that an exhaustive CSI acquisition procedure is still necessary from time to time to provide inputs to the developed prediction method. In contrast, our primary interest lies in evaluating and comparing the performance of using imperfect CSI directly, imperfect CSI with the support of an offline learning mechanism, and precise CSI. We aim to provide insight into the trade-off between CSI acquisition overhead and the achieved performance, serving as valuable guidance for satellite transceiver designers.

The summary of related works is presented in Table I. Based on the above survey results, we conclude that LEO satellite swarm-enabled distributed MIMO communications are not well investigated yet, failing to provide mature algorithms for current LEO SATCOM. Also, realistic considerations, such as the imperfect CSI effect, are also neglected in the literature. Thus, in this work, we start from an important topic of such systems in practice, the dynamic formation problem, to enable efficient and real-time LEO satellite swarm-enabled distributed MIMO communications. Moreover, we further evaluate the overheads of different formation methods and seek practical solutions to work with CSI imperfection and reduced overheads. Thus, the capacity of LEO satellite swarm-enabled distributed MIMO

Papers/Topics	Single LEO node	LEO constellations	SATCOM modeling	Imperfect CSI modeling
[14], [15], [17]–[23]	✓			
[24]–[26]	✓			✓
[16]		✓	✓	
Ours		√	√	√

TABLE I SUMMARY OF RELATED WORKS

communications can be increased and it is starting possible to transfer the aforementioned works into the considered scenario for improved transmission quality.

III. SYSTEM MODEL

In this section, we first introduce the unique channel behaviors of the considered LEO SATCOM to bring the motivation of utilizing satellite swarm to provide spatial diversity for MIMO use. Then we discuss how the geometrical relationships between the ground station and candidate satellites affect the channel behaviors of LEO SATCOM.

A. Uplink SATCOM Propagation Model

We consider a wireless communication system between a ground terminal with $N_{\rm T}$ antennas and $N_{\rm S}$ single-antenna candidate satellites. We further consider all candidate satellites are following trailing formation pattern [44] and operating in the same orbit (i.e., LEO). Let $\mathbf{H} = [\mathbf{h}_1, \mathbf{h}_2, \dots, \mathbf{h}_{N_{\rm S}}] \in \mathbb{C}^{N_{\rm S} \times N_{\rm T}}$ denotes the the communication channel and $\mathbf{h}_l = \in \mathbb{C}^{1 \times N_{\rm T}}$ represents the wireless communication channel between the ground station and l th satellite. The i th element of \mathbf{h}_l can be expressed by

$$\mathbf{H}_{l,i} = [\mathbf{h}_l]_i = \mathbf{h}_i^l = \frac{1}{\sqrt{L_i^l}} e^{-j(2\pi(f_c/c_0 + f_D^l)d_{l,i} + \phi_l)}, \quad (1)$$

where f_c is the carrier frequency, c_0 is the light speed, f_D^l is the Doppler frequency shift of each satellite, $d_{l,i}$ is the distance from the l-th satellite's to the i-th ground station antenna, and $\phi_l \in [0,2\pi]$ is a uniformly distributed phase shift of the l-th satellite caused by the atmosphere. Note that the Doppler frequency shift is caused by the high relative velocity between each satellite and ground station, and thus can be further expressed as $f_D^l = f_c \frac{\vec{v}_l}{c_0}$, where \vec{v}_l represents the relative velocity between ground station and l-th satellite. Moreover, L_i^l is the total attenuation loss, which is given in decibel as

$$L_{i|dB}^{l} = 20log_{10}(4\pi f_{c}d_{l,i}/c_{0}) + L_{sf,l} + L_{gas,l} + L_{ts,l}, \quad (2)$$

where $L_{{\rm sf},l}$ is the shadow fading, $L_{{\rm gas},l}$ describes atmospheric gas absorption, and $L_{{\rm ts},l}$ includes the losses due to tropospheric scintillation.

The satellite channel model described earlier exhibits two distinctive features that distinguish it from conventional mobile communications. These features motivate the development of specialized communication system designs that leverage these characteristics. Firstly, the satellite channel utilizes a pure line-of-sight (LoS) channel to propagate radio waves, as demonstrated by (1), which is consistent with recent literature and

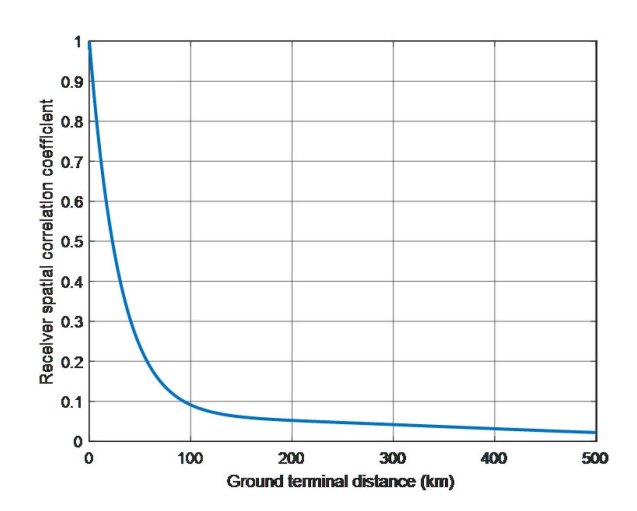


Fig. 1. Signal correlation from two ground stations with different ground station distance in downlink SATCOM.

real-world measurement reports [16], [45], [46], [47], [48], [49]. To explain, due to the high signal attenuation in this type of channel, the LoS signal component dominates the propagation mechanism in a satellite radio channel. Additionally, a report by the International Telecommunication Union (ITU) also confirms this tendency in the SATCOM downlink channel. The report highlights that maintaining an appropriate distance between two ground stations is crucial to enable the correlation of received signals from the same satellite, thus providing the necessary spatial diversity for further use. This relationship is depicted in Fig. 1, where the x-axis represents the distance between two ground stations and the y-axis indicates the resulting receiver spatial correlation coefficient. As shown in the figure, a spacing of at least several tens of kilometers between two ground stations is necessary to ensure the existence of spatial diversity in downlink SATCOM. If multiple antennas are configured within the same ground station, no spatial diversity can be utilized in such a communication system, as the received signals from those antennas will be identical. Similar trends are observed in uplink SATCOM scenarios described in (1), underscoring the need for a swarm structure to generate the required spatial diversity for MIMO use. In addition to the LoS channel discussed above, the satellite channel model also presents an unparalleled opportunity for system designers to utilize geo-information in the development of SATCOM systems. Unlike conventional mobile communications, which rely on statistical distribution to model the multipath effect, the random variables in the wireless communication channel between the ground station and the l th satellite are the atmospheric effect ϕ_l and shadow fading effect

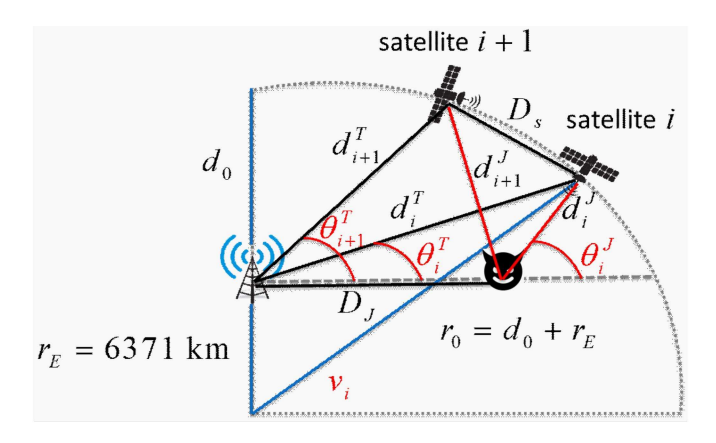


Fig. 2. Geometric relationship between the ground station and candidate satellites.

 $L_{\mathrm{sf},l}$. The other terms are determined by the satellite's trajectories (i.e., distance to the ground station $d_{l,i}$ and relative velocity to the ground station \vec{v}_l) and environment-defined constants (i.e., the operated carrier frequency f_c , atmospheric gas absorption $L_{\text{gas},l}$, and tropospheric scintillation $L_{ts,l}$). While these environmentdefined constants can be known as prior knowledge, the trajectories of the satellites are also easy to determine since they operate in a fixed orbit (i.e., LEO). Additionally, both the ground station and satellite swarm sides must seamlessly monitor precise physical attributes, such as longitude, latitude, height, velocity, and inter-satellite distance. Commercial satellite service providers, such as SpaceX and Amazon, have implemented Application Programming Interfaces (APIs) to facilitate this monitoring process. Utilizing the available geometrical information in the considered LEO SATCOM scenarios can aid in the design of transceiver operations, which is one of the major goals of this work.

B. Uplink SATCOM Using Swarm Structure

Furthermore, in this section, we aim to describe how geometric relationships between the ground station and candidate satellites affect the above channel model. Specifically, we consider an uplink SATCOM scenario as shown in Fig. 2. Following the Earth-centered coordinate system, we assume all satellites are operating in a LEO, where the distance to Earth center is fixed as r_0 . However, in realistic cases, ground terminal will be built on the Earth surface, thus, the distance between each satellite and the ground station will be different. In this paper, we assume that the inter-satellite distance between two adjacent satellites lth satellite and l+1th satellite is $D_{s;l,l+1}$ and the inter-satellite communications can be performed perfectly using optic communications. Next, given the distance from lth satellite and ground station as d_l , we aim to discuss how the inter-satellite distance $D_{s;l,l+1}$ affects the distance between l+1th satellite and ground station. To do so, we first analyze the geometric relationship of the considered LEO SATCOM system. Specifically, using the Earth-centered coordinate system, the polar coordinates of satellite l can be denoted as $\mathbf{r}_l = [r_0, v_l]$, where r_0 is the orbital radius and $v_l \in [0, 2\pi]$ is the polar angle. The ground station is located at position $\mathbf{r}_T = [r_E, \pi/2]$, where $r_E = 6371$ km is the Earth's radius, With the above setting, we aim to transfer the whole communication system into ground station-centered coordinate system to obtain geometry-based communication systems. Using the ground station-centered coordinate system, the polar coordinates of satellite l can be expressed as $\mathbf{d}_l = [d_l, \theta_l]$, where d_l is the distance between the ground station and satellite l, and $\theta_l \in [0,\pi]$ is the angle of departure (AoD) from the ground station to satellite l. In this setting, how geometric relationships between the ground station and candidate satellites affect the uplink SATCOM swarm channel model can be elegantly presented in the following corollaries.

Lemma 3.1: The distance d_l between satellite l and the ground station is given as $d_l = \sqrt{d_0^2 + 2r_E r_0(1 - \sin(v_l))}$.

Proof: Given a triangle with satellite i, the Earth's center, and the ground station, we have $(d_l)^2 = r_E^2 + r_0^2 - 2r_E r_0 \cos(\frac{\pi}{2} - v_l)$ via the law of cosines. Further, simplify this equation as below:

$$(d_l)^2 = r_E^2 + r_0^2 - 2r_E r_0 \cos(\frac{\pi}{2} - v_l)$$

$$= r_E^2 + r_0^2 - 2r_E r_0 \sin(v_l)$$

$$= (r_0 - r_E)^2 + 2r_E r_0 - 2r_E r_0 \sin(v_l)$$

$$= d_0^2 + 2r_E r_0 (1 - \sin(v_l)). \tag{3}$$

Thus, we obtain the result $d_l = \sqrt{d_0^2 + 2r_E r_0(1-\sin(v_l))}$. Lemma 3.2: The relationship between d_0 and d_{l+1} can be characterized by $D_{s;l,l+1}$ and described as $d_{l+1} = \sqrt{d_0^2 + 2r_E r_0(1-\sin(v_l+\arccos(1-D_{s;l,l+1}^2/2r_0^2)))}$.

Proof: We first consider a triangle with satellite l, satellite l+1, and the ground station, we have $D_{s;l,l+1}^2 = r_0^2 + r_0^2 - 2r_0r_0\cos(\Delta v)$ by denoting $\Delta v = v_{l+1} - v_l$ by the law of cosines. Through appropriate transpositions, we obtain $2r_0r_0\cos(\Delta v) = 2r_0^2 - D_{s;l,l+1}^2$. Thus, $\cos(\Delta v) = 1 - D_{s;l,l+1}^2/2r_0^2$ holds. Finally, we can represent the angle difference Δv between two adjacent satellites as a function of $D_{s;l,l+1}$, that is, $\Delta v = \arccos(1 - D_{s;l,l+1}^2/2r_0^2)$ Then, following the conclusion of Lemma III.1, we know that for satellite l+1, the equation $d_{l+1} = \sqrt{d_0^2 + 2r_E r_0(1 - \sin(v_{l+1}))}$ also holds. Further, simplify this equation and take the above conclusion into the equation as below:

$$\begin{split} d_{l+1} &= \sqrt{d_0^2 + 2r_E r_0 (1 - \sin(v_{l+1}))} \\ &= \sqrt{d_0^2 + 2r_E r_0 (1 - \sin(v_l + \Delta v))} \\ &= \sqrt{d_0^2 + 2r_E r_0 (1 - \sin(v_l + \arccos(1 - D_{s;l,l+1}^2 / 2r_0^2)))}. \end{split}$$

$$(4)$$

Note that d_l and θ_l are time variant, but r_0 and $r_{\rm E}$ are constant over time. All these values can be easily acquired or known as the priori at the ground station, since satellites are moving on predefined orbits. Now, the geometric relationships between the ground station and candidate satellites are clear and we demonstrate that $D_{s:l,l+1}$ can affect the SATCOM system by

influencing the distance from candidate satellites to the ground station.

Lemma 3.3: Let d_l be the distance from the ground station to satellite l, we denote the distance from the m th antenna of the ground station to satellite l as $d_{l,m}$ and the equation $d_{l,m} = d_l - D_A \cdot m \cdot \cos(\theta_l)$ holds, where $D_A = \frac{c_0}{2f_c}$ is the antenna spacing between two adjacent antennas in the ground station.

Proof: Given the distance from the ground station to satellite i as d_l , we now aim to analyze the distance from the m th antenna of the ground station to satellite l (i.e., $d_{l,m}$). By doing so, the transmitting signal difference between different antennas can be studied. First, due to the extremely long transmission distance nature of SATCOM, it is fair to assume the receive signal on the satellite side will present as a plane wave. Then, one can notice that, comparing with the first antenna (with reference distance d_l , i.e., m=0), the signal traveling distance from m th antenna of the ground station to satellite is reduced by $D_A \cdot m \cdot \cos(\theta_l)$. Thus, we obtain the result $d_{l,m} = d_l - D_A \cdot m \cdot \cos(\theta_l)$.

With the above lemmas, we can further express the channel matrix between the ground station to satellite \boldsymbol{l} as

$$\mathbf{h}_l = \alpha_l \mathbf{a}_l,\tag{5}$$

where \mathbf{a}_l is the steering vector following

$$\mathbf{a}_{l} = \left[e^{-j2\pi (f_{c}/c_{0} + f_{D}) \cdot D_{A} \cdot m \cdot \cos(\theta_{l})} \right]_{m=0}^{N_{T}-1}, \tag{6}$$

and α_l is the complex gain as $\alpha_l=\frac{1}{\sqrt{L^l}}e^{-j(2\pi(f_c/c_0+f_D)d_l+\phi_l)}$ described in (1).

IV. DYNAMIC LEO SATELLITE SWARM FORMATION

A. Problem Formulation

With the above system modeling, we introduce the interested dynamic formation problems in this section. We consider a SATCOM scenario, where a wireless communication system is built between a ground terminal with $N_{\rm T}$ antennas and a satellite swarm consisting $N_{\rm S}$ single-antenna satellites operating in the same trail. Assuming that the inter-satellite distance between two nearby satellites is a random variable following uniform distribution, our goal is to find out the most appropriate $N_{\rm R}$ satellites out of $N_{\rm S}$ satellites to form a wireless communication system with the highest communication capability. Mathematical speaking, the interested problem can be expressed as

subject to
$$\sum_{i=1}^{N_{\rm S}} s_i = N_{\rm R}, \tag{7}$$

where $H \in \mathbb{C}^{N_S \times N_T}$ is a channel matrix following the aforementioned SATCOM structure, λ is the operating signal-to-noise-ratio of the considered SATCOM system. Notably, the considered linear programming question is a NP-hard problem and our goal is to find the best formation result s by only connecting to N_R selected satellites for maximized capacity. s is the optimal formation results, where involved satellites are set as 1 and other satellites are set as 0.

B. Design Considerations

In this section, we introduce the procedures to utilize existing formation solutions in LEO SATCOM to discuss the design considerations of dynamic formation solutions. Given the considered scenario, where our goal is to find the best formation result s by selecting N_R satellites out of N_s candidating satellites for maximized capacity. During the pilot phase, the ground station transmits known pilots to all N_s candidating satellites for channel estimation purposes. Those $N_{\rm s}$ satellites then need to go through an exhaustive channel estimation procedure and provide feedback on the channel estimation results to the ground station, after which the dynamic formation process can begin, selecting a subset of satellites containing $N_{\rm R}$ satellites for wireless data connectivity (i.e., $N_R < N_s$ in a practical case.). While these procedures may work well for conventional mobile communications, there are two drawbacks that hinder their direct use in LEO SATCOM systems. Firstly, obtaining precise CSI in LEO SATCOM scenarios is noticeably costly, particularly for the CSI of all candidating satellites is required when only a subset will be used in the data transmission phase. Secondly, due to the high mobility of LEO satellites, the coherence time of the system is much shorter than conventional mobile communications. This makes the aforementioned resource-demanding CSI training procedures even more challenging, as they need to be performed continuously to update time-varying CSI throughout the transmission. Moreover, such a short coherence time also prohibits the use of computationally demanding dynamic formation methods. Based on the above reasons, we conclude that a desirable and practical dynamic formation solution should (i) be able to reduce the usage of precise CSI for the reduced signaling overhead and (ii) be able to provide real-time capabilities to be adopted in fast-moving LEO SATCOM scenarios. Thus, in the rest of this paper, we will develop a learning-based dynamic formation solution to achieve the aforementioned design considerations and intensive simulation results demonstrate that the proposed method can result in reduced signaling overhead and provide real-time operations to practical LEO SATCOM.

C. Imperfect CSI Estimation Models

In this paper, to achieve our goal of addressing the challenges of imperfect CSI in LEO SATCOM, we introduce two types of imperfect CSI models: geometric CSI estimation and conventional CSI estimation models. These models will be discussed in detail in the following sections.

1) Geometrical CSI Estimation Model: In this section, we propose a model to capture imperfect CSI solely based on the available geo-information for LEO SATCOM. Due to the strong LoS properties in LEO SATCOM channels, the resulting channel is strongly connected to the geometry of satellites, such as their location and speed. Additionally, for safety purposes, geo-information from satellites is required to be periodically reported to the ground station. Thus, with the understanding of LEO SATCOM, we propose the following model to capture imperfect CSI solely based on the available geo-information,

that is,

$$\hat{\mathbf{H}}_{l,i} = \frac{1}{\sqrt{\hat{L}_i^l}} e^{-j(2\pi(f_c/c_0 + f_D^l)d_{l,i})},\tag{8}$$

where L_i^l is the estimated total attenuation loss, which is given in decibel as

$$\hat{L}_{\text{ildB}}^{l} = 20log_{10}(4\pi f_c d_{l,i}/c_0) + L_{\text{gas},l} + L_{\text{ts},l}.$$
 (9)

Comparing with the original channel model in (1) and (2), one can notice that random terms, phase shift caused by the atmosphere ϕ_l and shadow fading attenuation loss $L_{\rm sf,l}$, are disregarded in the model, as they are dynamic and cannot be observed solely based on geo-information. Importantly, the proposed model does not require any channel training or feedback procedures, providing a practical solution to the challenges of acquiring precise CSI in LEO SATCOM scenarios, where acquiring precise CSI for all satellites can be costly and resource-intensive.

2) Conventional CSI Estimation Model: In the second type of imperfect CSI modeling, we consider the commonly used pilot-based channel estimation methods. The estimated channel obtained inevitably suffers from imprecision, which is related to the pilot-to-noise-ratio (PNR) [50], [51], [52]. In this type of imperfect CSI modeling, we define the imperfect channel matrix as:

$$\hat{\mathbf{H}}_{l,i} = \mathbf{H}_{l,i} + \Delta \mathbf{H}_{l,i;\text{iCSI}},\tag{10}$$

where each element of $\Delta \mathbf{H}_{l,i;i\text{CSI}}$ is an i.i.d. complex Gaussian with both zero mean and variance $\sigma_{i\text{CSI}}^2$. Different values of $\sigma_{i\text{CSI}}^2$ represent different levels of severity of CSI imperfection and can be simulated by considering different PNRs.

V. LEARNING-BASED DYNAMIC FORMATION

In this section, we present our proposed solution to address the interested integer programming problem in (7), which aims to enhance the current LEO SATCOM by generating recommended formation results with low overheads.

A. Overview

As discussed in the introduction, our approach leverages machine learning techniques to develop dedicated formation designs that can address both the algorithm deficit and model deficit challenges faced by LEO SATCOM. Our proposed method can provide real-time formation capability by offloading computationally demanding operations to the offline training process, which mitigates the algorithm deficit. More importantly, thanks to the pure LoS channel structure of the LEO SATCOM, the proposed method can work with imperfect CSI to mitigate signaling overheads, which addresses the model deficit. In our framework, we use coarse CSI generated by the geometrical CSI estimation, rather than precise CSI, as inputs to provide formation recommendations. Based on this input, the method can output the priority (i.e., selection probability) of each candidate satellite for further use. This recommendation (i.e., soft output) allows a small-scale brute force method to be employed to validate the formation results using only a portion of precise CSI and compensate for the performance loss due to the imperfect CSI if needed. A hyper-parameter (i.e., searching indicator) is provided to strike an optimal trade-off between achieved performance and acceptable signaling overhead. By doing so, the achieved performance can be maintained, and the signaling overhead of acquiring precise CSI can be significantly reduced. In the following sections, we will describe the development of our proposed method, discuss the specifics of the employed machine learning techniques, and explain how to deploy the method in real-world scenarios.

B. Dynamic Formation Based on Neural Network

To develop learning-based solutions for solving (7) in a supervised learning manner, a neural network will be trained as a classifier so that formation classification can be performed in the online inferring phase. To do so, one possible approach is to model the problem as a multi-class classification task with all possible formation cases, resulting in $C_{N_{\mathrm{R}}}^{N_{\mathrm{S}}}$ classes. However, several drawbacks will be raised by doing so. First, the underlying assumption of this solution is that all formation classes are mutually exclusive and independent, being not accurate to the considered problem. For example, the correlation between formation results with satellites $\{1, 2, 3, 4\}$ and $\{1, 2, 3, 5\}$ is obviously higher than that between formation results with satellites $\{1, 2, 3, 4\}$ and $\{7, 8, 9, 10\}$ since several satellites are selected in common in the first case. The multi-class classification assumption fails to account for the underlying correlation in the problem. Secondly, implementing a multi-class classification setting to the considered problem would require up to $C_{N_{\rm p}}^{N_{\rm S}}$ neurons to be used in the final layer of the neural network for outputting the classification results. In practical cases where $N_{\rm S}=25$ and $N_{\rm R}=4$, this would result in a final layer with 12650 neurons, which is a huge number. Furthermore, deploying such a large neural network would require ample training samples, making it challenging to use in real LEO SATCOM scenarios.

As an alternative, we provide an innovative solution, multilabel classification, to solve the considered question and avoid the aforementioned drawbacks. Mathematical speaking, the proposed method can be expressed as

$$f(\hat{\mathbf{H}}; \Theta^*) = \hat{\mathbf{s}},\tag{11}$$

where $\hat{\mathbf{H}} \in \mathbb{C}^{N_{\mathrm{S}} \times N_{\mathrm{T}}}$ is a imperfect CSI sample, $\hat{\mathbf{s}} \in \mathbb{R}^{N_{\mathrm{S}}}$ is the formation recommendations, and Θ^* is the optimal trainable parameters of neural network. Note that the proposed method differs from the traditional multi-class classification setting, which aims to predict the probability of a specific formation class. Instead, the proposed method predicts the probability of each satellite being selected to achieve maximized capacity, matching the original optimization problem in (7). By doing so, this approach reduces the number of neurons required from 12,650 to 25 in the practical case with $N_{\mathrm{S}} = 25$ and $N_{\mathrm{R}} = 4$, making it more feasible for deployment in real LEO SATCOM scenarios. In light of this direction, to train the proposed neural network by obtaining the optimal trainable parameters Θ^* , we

define the loss function below:

$$\underset{\Theta}{\text{minimize}} \ d(\hat{\mathbf{s}}, \mathbf{s}) = d(f(\hat{\mathbf{H}}; \Theta), \mathbf{s}). \tag{12}$$

where d(.) is the employed distance function so that the distance between ground truth s and prediction s can be minimized to achieve our goal. Recalling our aim is to provide probability meaning to the outputted formation recommendations s, we employ binary cross-entropy function as the distance function, expressed as:

$$d(f(\hat{\mathbf{H}}; \Theta), \mathbf{s}) = \sum_{i=1}^{N_{\mathbf{S}}} \mathbf{s}_{i} \log(\hat{\mathbf{s}}_{i}) + (1 - \mathbf{s}_{i}) \log(1 - \hat{\mathbf{s}}_{i}).$$
 (13)

By assigning binary cross-entropy function as the loss function to provide the probability meaning to the final output, note that in the ground truth s, if ith satellite is selected, the formation recommendations of ith satellite will need to be set as a larger probability (i.e., close to 1) and vice versa to minimize the employed binary cross-entropy function in (13). During this process, the employed neural network starts to learn to predict the formation results with the maximized capacity solely based on the inputted imperfect CSI. To further explain, in our considered channel modeling, various random fading factors, such as gas absorption loss, tropospheric scintillation loss, and shadowing fading loss, influence the behavior of satellite channels. While these random fading terms cannot be precisely recovered from an information theory perspective, a notable distinction from conventional mobile communications becomes apparent. That is, the dominant influence on satellite channel behavior stems from the geometric relationships between satellites and ground stations. This dominance arises due to the pure LoS channel type and the ultra-long transmission distances between satellites and ground stations. In essence, even solely considering these geometric relationships yields the fundamental "structure" of satellite communication channels. As a result, after training, the predicted probability of each satellite provides the priority to include this satellite in the final formation for the maximized capacity. Simulation results confirm that with the aid of the proposed neural network, certain performance improvements can be expected compared with only utilizing an imperfect CSI case.

C. Learning Specifics

Next, we provide details on the learning specifics of the proposed method, including the network architecture and hyperparameter settings. The input of the proposed method is the imperfect channel matrix \hat{H} , which is a $N_T \times N_S$ complexvalued matrix. To feed the complex-valued matrix into the neural network, we transform the channel matrix into the angle and amplitude form to allow real-valued processing of neural networks. Thus, the input layer of the proposed method is a real-valued vector of size $2N_SN_T \times 1$. Then, three hidden layers are employed to further process the given information, with the number of neurons 128, 64, and 32, respectively. In each layer, the ReLU function is employed as the activation function to provide non-linearity. Finally, the sigmoid function is employed

TABLE II IMPLEMENTATION DETAILS OF THE PROPOSED METHOD

Layer Name	Dimension	Activation	# of paras.	
Input Layer	$2N_{\rm S}N_{\rm T} \times 1$	N/A	0	
Dense Layer 1	128×1	ReLU	15488	
Dense Layer 2	64×1	ReLU	8256	
Dense Layer 3	32×1	ReLU	2080	
Output Layer	$N_{\rm S} imes 1$	Sigmoid	495	

Algorithm 1: Training Procedure of the Proposed Method.

Output: Optimal model weight Θ^*

- 1: Generate $H \in \mathbb{C}^{N_S \times N_T}$ and corresponding $\hat{\mathbf{H}} \in \mathbb{C}^{N_{\mathrm{S}} \times N_{\mathrm{T}}}$ based on system model
- 2: Prepare $C_{N_{\mathrm{R}}}^{N_{\mathrm{S}}}$ combinations denoted as $\{\mathbf{s}_{i}\}$, compute $C_{i} = \log \det(I_{N_{\mathrm{T}}} + \lambda \mathbf{H}^{H} \operatorname{diag}(\mathbf{s}_{i})\mathbf{H})$ for each $i = \{1, \ldots, C_{N_{\mathrm{S}}}^{N_{\mathrm{R}}}\}$ 3: Find $i^{*} = \operatorname{argmax}_{i}C_{i}$, setting $\mathbf{s} = \mathbf{s}_{i^{*}}$ as the label with
- involved satellites 1, others as 0
- Train the model via $\Theta^* = \min_{\Theta} d(f(\hat{H}; \Theta), s)$ in (11)

in the final layer to output probability predictions. Note that the employed ReLu and sigmoid function can be expressed as:

$$ReLU(z) = \begin{cases} z & \text{, if } z > 0, \\ 0, & \text{if } z \le 0, \end{cases}$$
 (14)

and

$$\operatorname{sigmoid}(z) = \frac{1}{1 + e^{-z}},\tag{15}$$

where z is the input real value. The neural network architecture is summarized in Table II for easy reference. As for other hyper-parameter settings, we utilize commonly used Adam as the optimizer with a learning rate of 0.001 to train the employed neural network for 30 epochs. The training, validation, and testing sets are with the size of 10000 non-overlapping samples. The early stopping technique is utilized to monitor the training process, ensuring the optimal trainable parameters are acquired. Simulation results demonstrate the proposed simple architecture is capable of providing the required learning capability and offers an attractive trade-off between computational complexity and achieved performance.

D. Deployment of the Proposed Method in Real Scenarios

Finally, we explain how to apply the proposed method to real LEO SATCOM scenarios to conclude this section. In the offline training stage, we collect precise CSI from the ground station to all candidate satellites and utilize the geometrical CSI estimation method to obtain imperfect CSI. Then the capacity of each possible formation combination is computed using precise CSI to generate a sample pair containing an imperfect CSI sample and the optimal formation result (i.e., label). After gathering sufficient samples, we utilize the proposed training framework and the defined loss function in (13) to obtain the optimal trainable parameters and complete the offline training stage. The entire process is outlined in Algorithm 1. In the online

Algorithm 2: Testing Procedure of the Proposed Method.

Input: Optimal model weight Θ^* , searching indicator k **Output:** Recommended formation result \tilde{s}_{j^*}

- 1: Given an imperfect CSI sample $\hat{\mathbf{H}} \in \mathbb{C}^{N_{\mathrm{S}} \times N_{\mathrm{T}}}$, generate formation recommendations as $f(\hat{H}; \Theta^*) = \hat{s}$
- Access the candidate satellites with the $N_{\rm R}+k$ highest probabilities based on s to obtain precise CSI
- partial matrix $\tilde{\mathbf{H}} \in \mathbb{C}^{(N_{\mathrm{R}}+k)\times N_{\mathrm{T}}}$ 3: Prepare $C_{N_{\mathrm{R}}}^{N_{\mathrm{R}}+k}$ combinations denoted as $\{\tilde{\mathbf{s}}_j\}$, compute $C_j = \log \det(I_{N_{\mathrm{T}}} + \lambda \tilde{\mathbf{H}}^H \operatorname{diag}(\tilde{\mathbf{s}}_j)\tilde{\mathbf{H}})$ for each $j = \{1, \ldots, C_{N_{\mathrm{R}}}^{N_{\mathrm{R}}+k}\}$ 4: Find $j^* = \operatorname{argmax}_j C_j$, output corresponding
- formation result § i*

testing stage, it is worth considering that LEO satellites exhibit high mobility and may swiftly move out of the coverage area of a terrestrial ground station within minutes. To address this challenge, we propose conducting the inference procedure on the terrestrial ground station side. By doing so, LEO satellites can passively participate in the proposed framework upon request, thus relieving them of the computational burden. To do so, firstly, the ground station will send out a connection request to all LEO satellites in the sky, and then those satellites will reply with their geometrical information if they have the capacity to build wireless connectivity with the ground station. By feeding an imperfect CSI based on the geometrical CSI estimation into the trained model with the optimal weight, the probability of selecting each satellite is predicted. Based on this recommendation and the given searching indicator, we only access the candidate satellites with the $N_{\rm R}+k$ highest probabilities, conducting a conventional CSI estimation procedure to obtain precise CSI. Then, a small-scale brute force method is performed to validate the capacity of all $C_{N_{\mathrm{R}}}^{N_{\mathrm{R}}+k}$ combinations, and the formation with the highest capacity during this validation process is output as the final formation recommendation. The entire process is outlined in Algorithm 2. Note that instead of accessing the full precise CSI matrix as in existing formation methods, we only access a partial matrix, thereby reducing the signaling overhead. Furthermore, instead of computing $C_{N_{\mathrm{R}}}^{N_{\mathrm{S}}}$ combinations as with conventional brute force methods, we only validate $C_{N_{\mathrm{R}}}^{N_{\mathrm{R}}+k}$ combinations thanks to the recommendations of the proposed neural network, which reduces the computational complexity. Simulation results suggest that considerable signaling overhead and computational complexity can be saved while maintaining satisfactory performance by using an appropriate setting for the search indicator k.

VI. PERFORMANCE EVALUATION

In this section, we provide simulation results to demonstrate the superiority of the proposed formation method and the adaptability to realistic SATCOM scenarios. We consider three different scenarios to evaluate the effectiveness of our method. In the first scenario, we utilize geometrical CSI information to provide imperfect CSI for formation purposes. In the second scenario, we use imperfect CSI obtained from conventional estimation methods to validate the generalization capability of our proposed learning formation method. Finally, in the third scenario, we consider a normal case where perfect CSI is available to investigate the behavior of our proposed method. These scenarios enable us to thoroughly evaluate the performance of our method in different contexts and demonstrate its versatility. In different scenarios, we compare our results with four different formation methods as below:

- Brute force using CSI: In this formation method, it is assumed that the ground station has access to precise CSI information. As a result, the capacity of each potential formation can be computed, and the one with the highest performance metric can be chosen as the swarm formation. This method provides optimal performance and serves as an upper bound for the problem being considered.
- Brute force using iCSI: In this formation method, we assume that only imperfect CSI is available at the ground station. An exhaustive search is still performed to obtain formation results, but due to the imperfect CSI, a performance loss compared to Brute Force CSI can be observed. This formation method provides an upper bound for the considered problem when only using imperfect CSI.
- Equal spacing: In this formation method, we adopt the approach proposed in [16] and aim to determine an optimal swarm formation based on inter-satellite distance alone. To do so, a swarm formation is created by selecting satellites with specific orders to achieve the largest inter-satellite distance statistically.
- Random: In this formation method, formation results will be chosen randomly to present the achieved performance without any designs.

As for the performance and overhead indicators, we employ the indicators below:

- Normalized spectrum efficiency: Given a group of candidate satellites operating in the LEO, we use the brute force method with precise CSI to obtain the optimal result with the highest capacity. The normalized spectrum efficiency of a method is defined as the ratio of the achieved spectrum efficiency of the method to the optimal spectrum efficiency. A higher normalized spectrum efficiency implies that the method can achieve a higher throughput connectivity.
- Computation formation overhead: We measure the computation formation overhead of each method by recording their running time in milliseconds (ms). A method with a shorter running time implies lower computational complexity and allows for longer data transmission phases, which can potentially improve the throughput of LEO SATCOM.
- Communication formation overhead: Given the high cost of acquiring precise CSI in LEO SATCOM, we measure the efficiency of each formation method by computing the ratio of utilized precise CSI to total precise CSI. For example, in a scenario with $N_{\rm S}=20$ candidate satellites, if a method can generate formation results by only utilizing precise CSI for 5 of these satellites, its communication formation overhead will be defined as 25%. This metric quantifies

Parameter	Value	
Carrier frequency (f_c)	1 GHz	
Number of antennas	4	
of ground terminal $(N_{\rm T})$	4	
Number of selected satellites (N_R)	4	
Orbit altitude (d_0)	446 km	
Satellite orbital velocity (\vec{v}_l)	7.64 km/s	
Inter-satellite distance $(D_{s;l,l+1})$	U(5,60)	
Shadowing fading loss $(L_{\rm sf}, l)$	N(0,4)	
Atmosphere gas absorption (L_{gas}, l)	0	
Tropospheric scintillation (L_{ts}, l)	27.5	
Noise temperature	300 K	
Noise power	-120 dBW	

TABLE III
PARAMETER SETTINGS FOR LEO SATCOM SCENARIO USING LINK 16 BAND

the amount of signaling overhead that can be saved by not utilizing precise CSI for the remaining candidate satellites. A lower communication formation overhead implies greater savings in signaling overhead during CSI training and feedback.

A. Dynamic Formation Using Imperfect CSI (Geometric CSI Estimation)

In this simulation, we consider LEO satellite swarm-enabled distributed MIMO communications in the Link-16 band, using the system model and detailed settings outlined in Table III. To study the behavior of different formation methods, we set the number of candidate satellites as $N_{\rm S}=15,20,25$. It's worth noting that we employ geometrical CSI estimation, which allows us to generate coarse CSI without any signaling overheads. The x-axis of Fig. 3 represents the transmit power of the ground terminal in dBW units, while the y-axis reports the normalized spectrum efficiency of different methods. In Fig. 3(a), we observe that random formation can only achieve 63.94% of full capacity in low transmit power regions. However, it can provide 91.66% of full capacity in high transmit power regions. This phenomenon reflects the fact that the considered dynamic formation problem is particularly important in low transmit power regions, where power resources are limited and need to be carefully allocated. We also notice that the brute force method, which uses imperfect CSI, can only result in 78.36% of full capacity in low transmit power regions. This suggests that imperfect CSI significantly affects the performance of formation methods.

Using only imperfect CSI, our proposed method can provide 74.28% of full capacity in low transmit power regions, which is comparable to the brute force method using imperfect CSI and outperforms equal spacing and random formation methods. By accessing the CSI from the ground station and satellites with top-6 probabilities (i.e., learning-based iCSI (k=2)), a small-scale brute force method can be applied, resulting in 85.74% achieved performance and a significant improvement of 10.46% compared to the brute force method. The hyper-parameter k can be flexibly adjusted according to the desired performance and

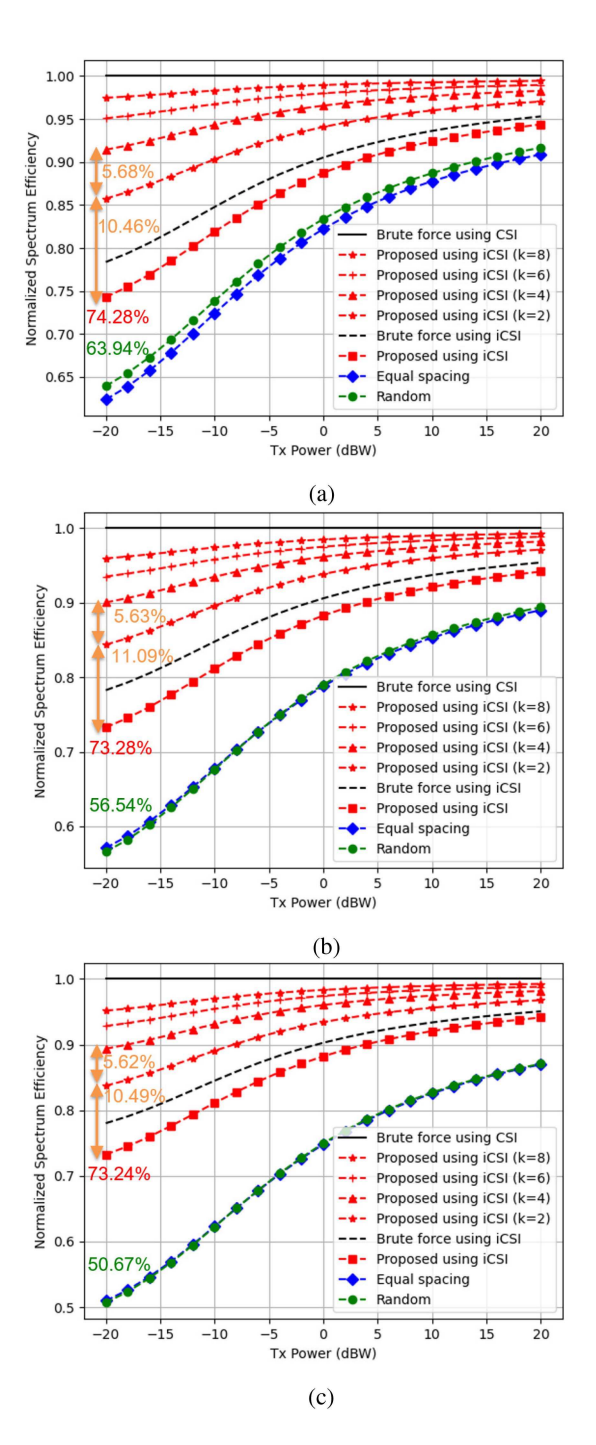


Fig. 3. Achieved normalized spectrum efficiency using different formation methods with geometrical CSI estimation scenario, (a) $N_{\rm S}=15$, (b) $N_{\rm S}=20$, (c) $N_{\rm S}=25$.

allowable signaling overheads and computational complexity. For example, with k=4, our proposed method achieves an additional 5.68% performance gain compared to the k=2 case, providing 91.41% of full capacity in the considered scenario. While the performance of using imperfect CSI may not satisfy all SATCOM applications, and the overheads of using perfect CSI are too costly in the considered scenario, our proposed method strikes a better trade-off between these two methods to provide

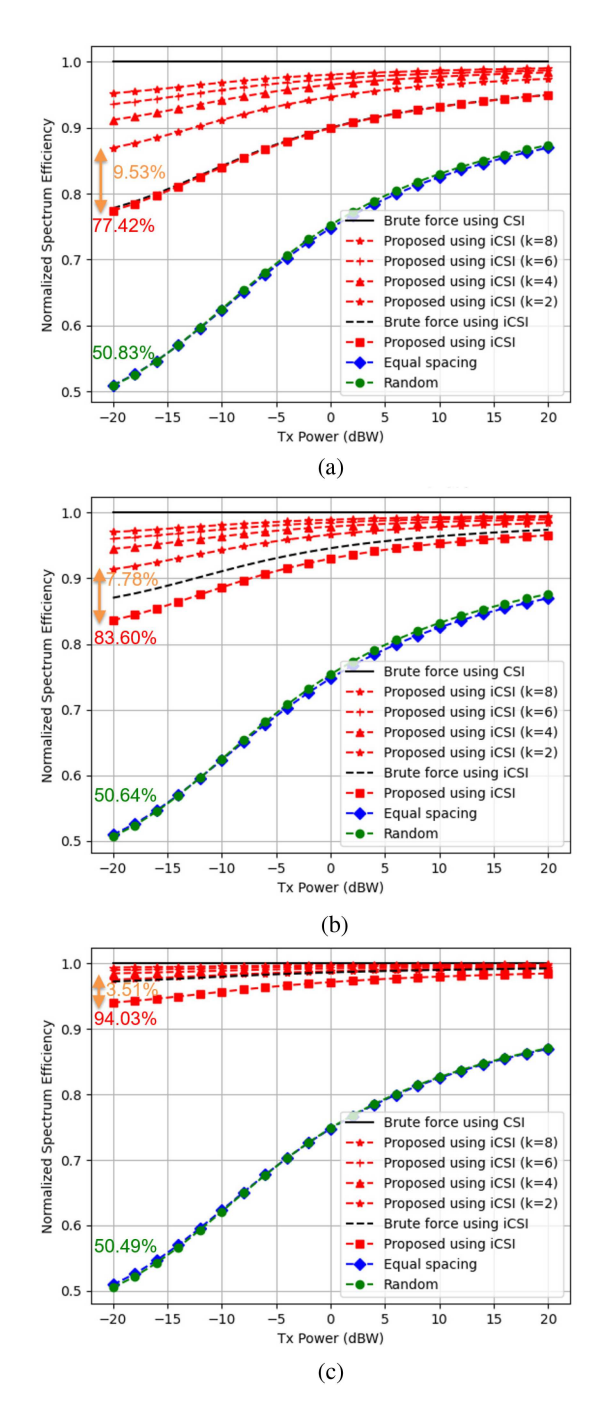


Fig. 4. Achieved normalized spectrum efficiency using different formation methods with conventional CSI estimation scenario, (a) $N_{\rm S}=25$ and PNR = 0 dB, (b) $N_{\rm S}=25$ and PNR = 10 dB, (c) $N_{\rm S}=25$ and PNR = 20 dB.

benefits. We also note that the equal spacing formation method can only provide similar performance to the random formation method, as it only utilizes inter-satellite distance to obtain the formation result, failing to consider the complex nature of LEO SATCOM. Similar tendencies and conclusions can be observed in Fig. 3(b) and (c), demonstrating the superiority and adaptability of our proposed formation method to realistic SATCOM scenarios. As a result, a consistent additional performance gain of about 10.5% and 5.6% can be achieved across different $N_{\rm S}$

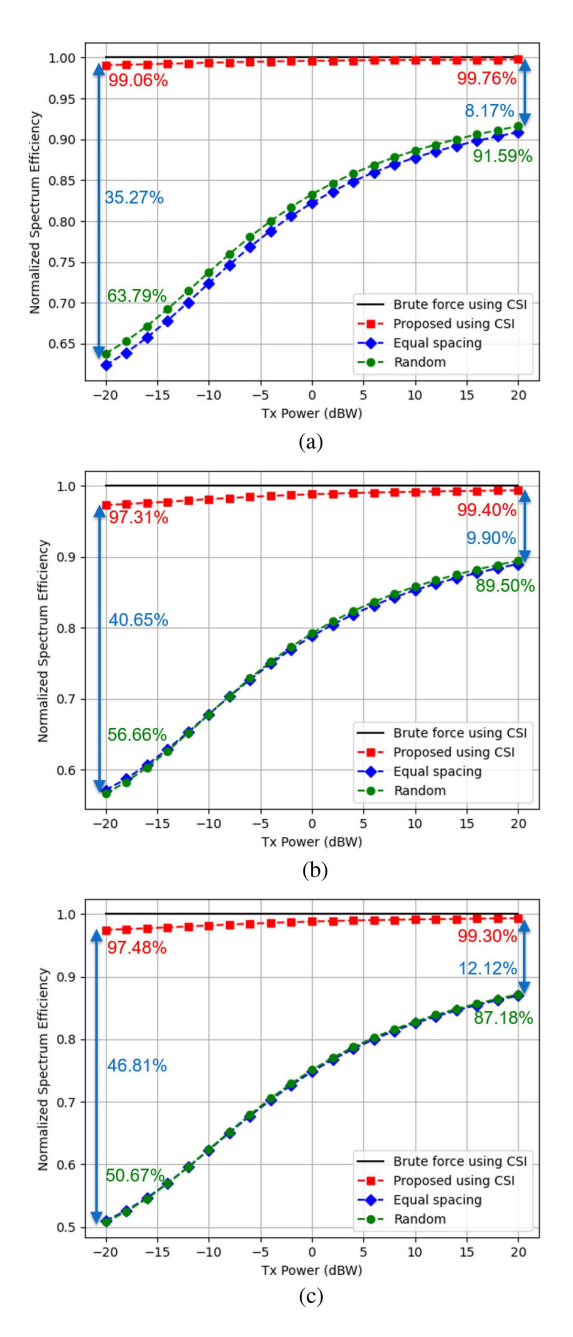


Fig. 5. Achieved normalized spectrum efficiency using different formation methods with perfect CSI estimation scenario, (a) $N_{\rm S}=15$, (b) $N_{\rm S}=20$, (c) $N_{\rm S}=25$.

scenarios. Furthermore, the gap between our proposed method and random formation increases with $N_{\rm S}$, suggesting that our proposed formation will be even more beneficial when more candidate LEO satellites can be chosen to form a swarm.

B. Dynamic Formation Using Imperfect CSI (Conventional CSI Estimation)

In this section, we compare the performance of the proposed method and other formation methods in scenarios where conventional CSI estimation methods are used. The number of candidate satellites is set to 25. The results shown in Fig. 4 reveal that the behavior of different formation methods is similar to

Formation overheads	$N_{\rm S} = 15$		$N_{\rm S} = 20$		$N_{\rm S} = 25$	
	Communication	Computation	Communication	Computation	Communication	Computation
	overhead	overhead	overhead	overhead	overhead	overhead
Brute force using CSI	15 (100%)	31.972 (100%)	20 (100%)	112.918 (100%)	25 (100%)	294.617 (100%)
Proposed (k = 6)	10 (66.67%)	4.946 (15.46%)	10 (50%)	4.921 (4.35%)	10 (40%)	4.901 (1.66%)
Proposed (k = 4)	8 (53.33%)	1.667 (5.21%)	8 (40.00%)	1.659 (1.46%)	8 (32.00%)	1.652 (0.56%)
Proposed (k = 2)	6 (40.00%)	0.379 (1.11%)	6 (30.00%)	0.377 (0.33%)	6 (24.00%)	0.377 (0.12%)
Brute force using iCSI	0 (0%)	31.972 (100%)	0 (0%)	112.918 (100%)	0 (0%)	294.617 (100%)
Proposed	0 (0%)	0.028 (0.08%)	0 (0%)	0.028 (0.02%)	0 (0%)	0.029 (0.009%)
Random	0 (0%)	0.008 (0.02%)	0 (0%)	0.008 (0.007%)	0 (0%)	0.008 (0.002%)

TABLE IV Formation Overheads of Different Formation Methods With Different $N_{\rm S}$

that observed in the previous simulations using geometrical CSI estimation, even with different PNRs. In low PNR cases (i.e., Fig. 4(a)), the gap between the brute force method using imperfect CSI and the proposed method is negligible. The proposed method can learn the mapping from imperfect CSI to precise CSI to aid the formation decision, making it especially useful when the CSI estimation quality is poor. However, in scenarios where the CSI estimation quality is good, the brute force method using imperfect CSI can still provide a slight performance gain since the correction capability of the proposed method still has its limitations, as shown in Fig. 4(b) and (c). We also observe that the behaviors of the proposed method are similar in Figs. 3(c) and 4(a), suggesting that the developed geometrical CSI estimation can provide similar CSI estimation results with PNR = 0 dB for formation purposes. Therefore, the geometrical CSI estimation can be employed in the considered dynamic formation problem to provide useful coarse CSI to trigger the proposed method without any signaling overheads. Finally, in Fig. 4(c), we demonstrate the capability of the proposed method in scenarios where highly precise CSI is available, achieving 94.03% of full capacity. Overall, the proposed method outperforms other formation methods in various scenarios, demonstrating its adaptability and superiority in LEO satellite swarm-enabled distributed MIMO communications.

C. Dynamic Formation Using Perfect CSI

In addition, we also considered a scenario where precise CSI is available at the ground station. This scenario is equivalent to the case where the PNR approaches infinity PNR $\rightarrow \infty$. As shown in Fig. 5(a), the proposed method outperforms existing methods by 35.27%, achieving 99.06% of full capacity. Even in the more challenging scenarios depicted in Fig. 5(b) and (c), where the number of candidate satellites increases, the gap between the proposed method and existing methods continues to grow. This finding highlights the advantages of using the proposed method when more candidate LEO satellites are available to form a swarm.

D. Formation Overhead Discussions

Finally, we consider the formation overheads for different formation methods, and provide a detailed comparison of communication and computation overheads in Table IV. In Table IV, we can see that no communication overhead is needed for the brute

force using iCSI, equal spacing, and random formation methods for different $N_{\rm S}$ cases. This is because these algorithms can take imperfect CSI obtained by geometrical CSI estimation without the need for CSI training and feedback procedures as inputs. However, the brute force using CSI method requires demanding communication overhead in the considered scenarios since precise CSI from the ground station to all candidate satellites is needed. While the brute force using iCSI method cannot deliver satisfying performance, and the communication overhead of brute force using CSI method is too demanding for LEO satellite swarm-enabled distributed MIMO communications scenarios, the proposed method can fit different communication overhead requirements by adjusting the hyper-parameter k, and provide superior performance compared to existing formation methods. Using the proposed method with k=2 in the $N_S=15$ case, only 40% communication overhead of the brute force using CSI method is needed since only the precise CSI of selected candidate satellites with higher priorities is needed, rather than the precise CSI of all candidate satellites. Furthermore, for a larger number of candidate satellites (i.e., $N_{\rm S}=25$), the needed communication overhead can be decreased to 24% compared to the brute force method. This is because the proposed method can always select potential candidate satellites and assign them higher priorities, making it even more efficient when serving large-scale swarms.

Regarding the computation overhead, we provide a detailed comparison in Table IV. The brute force methods, both using iCSI and CSI, require 31.972 ms to obtain the formation results in the $N_{\rm S}=15$ case, which violates the real-time processing requirements in the considered LEO satellite swarm-enabled distributed MIMO communications scenarios. Additionally, when the number of candidate satellites increases, the computation time increases exponentially, reaching 112.918 ms ($N_S = 20$ case) and 294.617 ms ($N_{\rm S}=25$ case). Recent literature reports that the coherence time of the considered LEO satellite swarm-enabled distributed MIMO communications scenarios is only 300 ms, making the execution of such methods impractical in real scenarios. In contrast, even considering the proposed method with k = 6, the most complicated but superiorperforming method, the computation overhead is still less than 5 ms, satisfying the real-time processing requirements in most communication systems. Moreover, even with a larger number of candidate satellites, the computation overhead will not increase, as the number of selected candidate satellites remains the same,

resulting in a reduced ratio compared to the computation overhead of the brute force (CSI) method (i.e., from 15.46% with $N_{\rm S}=15$ to 1.66% with $N_{\rm S}=25$). This phenomenon suggests that the proposed method becomes more efficient when serving large-scale swarms. In conclusion, considering the trade-off between performance and needed overheads, the simulation results demonstrate the effectiveness of the proposed method, especially when serving large-scale swarms with strict overhead requirements.

VII. CONCLUSION

To address the deficits in both model and algorithm in existing methods for LEO satellite swarm-enabled distributed MIMO communications, we propose a novel learning-based formation method. Our approach utilizes geometrical CSI estimation to provide effective coarse CSI for formation purposes without incurring any signaling overheads, thanks to the geometrical relationship understanding between the ground station and candidate satellites. Using the recommendations produced by our method, we only require a portion of precise CSI for the validation process, which significantly reduces the signaling overheads in LEO satellite swarm-enabled distributed MIMO communications. Our simulation results demonstrate that our real-time formation method can help maintain performance and reduce formation overheads in LEO satellite swarm-enabled distributed MIMO communications, especially in low-transmit power regions and large-swarm scenarios. As for future work, we aim to introduce unsupervised or self-supervised training methods to avoid the labeling costs of our proposed formation method in the offline training stage. Additionally, we will refine our proposed geometrical CSI estimation approach to further expand its usage in LEO satellite swarm-enabled distributed MIMO communications.

REFERENCES

- M. Z. Chowdhury, M. Shahjalal, S. Ahmed, and Y. M. Jang, "6G wireless communication systems: Applications, requirements, technologies, challenges, and research directions," *IEEE Open J. Commun. Soc.*, vol. 1, pp. 957–975, 2020.
- [2] W. Saad, M. Bennis, and M. Chen, "A vision of 6G wireless systems: Applications, trends, technologies, and open research problems," *IEEE Netw.*, vol. 34, no. 3, pp. 134–142, May/Jun. 2020.
- [3] C. De Alwis et al., "Survey on 6G frontiers: Trends, applications, requirements, technologies and future research," *IEEE Open J. Commun. Soc.*, vol. 2, pp. 836–886, 2021.
- [4] W. Jiang, B. Han, M. A. Habibi, and H. D. Schotten, "The road towards 6G: A comprehensive survey," *IEEE Open J. Commun. Soc.*, vol. 2, pp. 334–366, 2021.
- [5] S. Dang, O. Amin, B. Shihada, and M.-S. Alouini, "What should 6G be?," Nature Electron., vol. 3, no. 1, pp. 20–29, 2020.
- [6] F. Rinaldi et al., "Non-terrestrial networks in 5G & Beyond: A survey," IEEE Access, vol. 8, pp. 165178–165200, 2020.
- [7] X. Lin, S. Rommer, S. Euler, E. A. Yavuz, and R. S. Karlsson, "5G from space: An overview of 3GPP non-terrestrial networks," *IEEE Commun. Standards Mag.*, vol. 5, no. 4, pp. 147–153, Dec. 2021.
- [8] M. M. Azari et al., "Evolution of non-terrestrial networks from 5G to 6G: A survey," *IEEE Commun. Surveys Tuts.*, vol. 24, no. 4, pp. 2633–2672, Fourthquarter 2022.
- [9] M. Giordani and M. Zorzi, "Non-terrestrial networks in the 6G era: Challenges and opportunities," *IEEE Netw.*, vol. 35, no. 2, pp. 244–251, Mar./Apr. 2021.

- [10] G. Araniti, A. Iera, S. Pizzi, and F. Rinaldi, "Toward 6G non-terrestrial networks," *IEEE Netw.*, vol. 36, no. 1, pp. 113–120, Jan./Feb. 2022.
- [11] Y. Zeng, R. Zhang, and T. J. Lim, "Wireless communications with unmanned aerial vehicles: Opportunities and challenges," *IEEE Commun. Mag.*, vol. 54, no. 5, pp. 36–42, May 2016.
- [12] X. Sun, D. W. K. Ng, Z. Ding, Y. Xu, and Z. Zhong, "Physical layer security in UAV systems: Challenges and opportunities," *IEEE Wireless Commun.*, vol. 26, no. 5, pp. 40–47, Oct. 2019.
- [13] Z. Yao, W. Cheng, W. Zhang, and H. Zhang, "Resource allocation for 5G-UAV-based emergency wireless communications," *IEEE J. Sel. Areas Commun.*, vol. 39, no. 11, pp. 3395–3410, Nov. 2021.
- [14] K.-X. Li et al., "Downlink transmit design for massive MIMO LEO satellite communications," *IEEE Trans. Commun.*, vol. 70, no. 2, pp. 1014–1028, Feb. 2022.
- [15] L. You, K.-X. Li, J. Wang, X. Gao, X.-G. Xia, and B. Ottersten, "Massive MIMO transmission for leo satellite communications," *IEEE J. Sel. Areas Commun.*, vol. 38, no. 8, pp. 1851–1865, Aug. 2020.
- [16] M. Röper, B. Matthiesen, D. Wübben, P. Popovski, and A. Dekorsy, "Beamspace MIMO for satellite swarms," in *Proc. IEEE Wireless Commun. Netw. Conf.*, 2022, pp. 1307–1312.
- [17] D. Zhou, M. Sheng, Y. Wang, J. Li, and Z. Han, "Machine learning-based resource allocation in satellite networks supporting internet of remote things," *IEEE Trans. Wireless Commun.*, vol. 20, no. 10, pp. 6606–6621, Oct. 2021.
- [18] P. V. R. Ferreira et al., "Reinforcement learning for satellite communications: From leo to deep space operations," *IEEE Commun. Mag.*, vol. 57, no. 5, pp. 70–75, May 2019.
- [19] M. Á. Vázquez et al., "Machine learning for satellite communications operations," *IEEE Commun. Mag.*, vol. 59, no. 2, pp. 22–27, Feb. 2021.
- [20] Z. Lin, M. Lin, T. D. Cola, J.-B. Wang, W.-P. Zhu, and J. Cheng, "Supporting IoT with rate-splitting multiple access in satellite and aerial-integrated networks," *IEEE Internet Things J.*, vol. 8, no. 14, pp. 11123–11134, Jul. 2021.
- [21] Z. Lin et al., "SLNR-based secure energy efficient beamforming in multibeam satellite systems," *IEEE Trans. Aerosp. Electron. Syst.*, vol. 59, no. 2, pp. 2085–2088, Apr. 2023.
- [22] K. An, M. Lin, J. Ouyang, and W.-P. Zhu, "Secure transmission in cognitive satellite terrestrial networks," *IEEE J. Sel. Areas Commun.*, vol. 34, no. 11, pp. 3025–3037, Nov. 2016.
- [23] Z. Lin, M. Lin, B. Champagne, W.-P. Zhu, and N. Al-Dhahir, "Secrecy-energy efficient hybrid beamforming for satellite-terrestrial integrated networks," *IEEE Trans. Commun.*, vol. 69, no. 9, pp. 6345–6360, Sep. 2021.
- [24] Y. Zhang, Y. Wu, A. Liu, X. Xia, T. Pan, and X. Liu, "Deep learning-based channel prediction for LEO satellite massive MIMO communication system," *IEEE Wireless Commun. Lett.*, vol. 10, no. 8, pp. 1835–1839, Aug. 2021.
- [25] G.-Y. Chang, C.-K. Hung, and C.-H. Chen, "A CSI prediction scheme for satellite-terrestrial networks," *IEEE Internet Things J.*, vol. 10, no. 9, pp. 7774–7785, May 2023.
- [26] Y. Zhang, A. Liu, P. Li, and S. Jiang, "Deep learning (DL)-based channel prediction and hybrid beamforming for LEO satellite massive MIMO system," *IEEE Internet Things J.*, vol. 9, no. 23, pp. 23705–23715, Dec. 2022.
- [27] A. Adhikary, H. C. Papadopoulos, S. A. Ramprashad, and G. Caire, "Multi-user MIMO with outdated CSI: Training, feedback and scheduling," in *Proc.* 49th Annu. Allerton Conf. Commun., Control, Comput., 2011, pp. 886–893.
- [28] J.-C. Shen, J. Zhang, E. Alsusa, and K. B. Letaief, "Compressed CSI acquisition in FDD massive MIMO: How much training is needed?," *IEEE Trans. Wireless Commun.*, vol. 15, no. 6, pp. 4145–4156, Jun. 2016.
- [29] C.-K. Wen, W.-T. Shih, and S. Jin, "Deep learning for massive MIMO CSI feedback," *IEEE Wireless Commun. Lett.*, vol. 7, no. 5, pp. 748–751, Oct. 2018
- [30] T. Wang, C.-K. Wen, S. Jin, and G. Y. Li, "Deep learning-based CSI feedback approach for time-varying massive MIMO channels," *IEEE Wireless Commun. Lett.*, vol. 8, no. 2, pp. 416–419, Apr. 2019.
- [31] B. Tolba, M. Elsabrouty, M. G. Abdu-Aguye, H. Gacanin, and H. M. Kasem, "Massive MIMO CSI feedback based on generative adversarial network," *IEEE Commun. Lett.*, vol. 24, no. 12, pp. 2805–2808, Dec. 2020.
- [32] G. Zhu, D. Liu, Y. Du, C. You, J. Zhang, and K. Huang, "Toward an intelligent edge: Wireless communication meets machine learning," *IEEE Commun. Mag.*, vol. 58, no. 1, pp. 19–25, Jan. 2020.
- [33] T. Erpek, T. J. O'Shea, Y. E. Sagduyu, Y. Shi, and T. C. Clancy, "Deep learning for wireless communications," in *Development and Analysis of Deep Learning Architectures*, Berlin, Germany: Springer, 2020, pp. 223–266.

- [34] L. Dai, R. Jiao, F. Adachi, H. V. Poor, and L. Hanzo, "Deep learning for wireless communications: An emerging interdisciplinary paradigm," *IEEE Wireless Commun.*, vol. 27, no. 4, pp. 133–139, Aug. 2020.
- [35] M. E. Morocho-Cayamcela, H. Lee, and W. Lim, "Machine learning for 5G/B5G mobile and wireless communications: Potential, limitations, and future directions," *IEEE Access*, vol. 7, pp. 137184–137206, 2019.
- [36] S. Ali et al., "6G white paper on machine learning in wireless communication networks," 2020, arXiv:2004.13875.
- [37] N. Farsad and A. Goldsmith, "Detection algorithms for communication systems using deep learning," 2017, arXiv:1705.08044.
- [38] S. Mohamed, J. Dong, A. R. Junejo, and D. C. Zuo, "Model-based: End-to-end molecular communication system through deep reinforcement learning auto encoder," *IEEE Access*, vol. 7, pp. 70279–70286, 2019.
- [39] C.-H. Lin et al., "GCN-CNVPs: Novel method for cooperative neighboring vehicle positioning system based on graph convolution network," *IEEE Access*, vol. 9, pp. 153429–153441, 2021.
- [40] J. Guo, C.-K. Wen, S. Jin, and G. Y. Li, "Convolutional neural network-based multiple-rate compressive sensing for massive MIMO CSI feedback: Design, simulation, and analysis," *IEEE Trans. Wireless Commun.*, vol. 19, no. 4, pp. 2827–2840, Apr. 2020.
- [41] Y.-C. Lin, Z. Liu, T.-S. Lee, and Z. Ding, "Deep learning phase compression for MIMO CSI feedback by exploiting FDD channel reciprocity," *IEEE Wireless Commun. Lett.*, vol. 10, no. 10, pp. 2200–2204, Oct. 2021.
- [42] Y.-C. Lin, T.-S. Lee, and Z. Ding, "Deep learning for partial MIMO CSI feedback by exploiting channel temporal correlation," in *Proc. 55th Asilomar Conf. Signals, Syst., Comput.*, 2021, pp. 345–350.
- [43] C.-H. Lin, S.-C. Lin, and E. Blasch, "Tulvcan: Terahertz ultra-broadband learning vehicular channel-aware networking," in *Proc. IEEE Conf. Com*put. Commun. Workshops, 2021, pp. 1–6.
- [44] R. Radhakrishnan, W. W. Edmonson, F. Afghah, R. M. Rodriguez-Osorio, F. Pinto, and S. C. Burleigh, "Survey of inter-satellite communication for small satellite systems: Physical layer to network layer view," *IEEE Commun. Surveys Tuts.*, vol. 18, no. 4, pp. 2442–2473, Fourthquarter 2016.
- [45] M. Röper, B. Matthiesen, D. Wübben, P. Popovski, and A. Dekorsy, "Distributed downlink precoding and equalization in satellite swarms," 2022, arXiv:2205.11180.
- [46] P.-D. Arapoglou, K. Liolis, M. Bertinelli, A. Panagopoulos, P. Cottis, and R. D. Gaudenzi, "MIMO over satellite: A review," *IEEE Commun. Surv. Tut.*, vol. 13, no. 1, pp. 27–51, Firstquarter 2011.
- [47] R. Schwarz, A. Knopp, B. Lankl, D. Ogermann, and C. Hofmann, "Optimum-capacity MIMO satellite broadcast system: Conceptual design for los channels," in *Proc. 4th Adv. Satell. Mobile Syst.*, 2008, pp. 66–71.
- [48] C. A. Hofmann, R. T. Schwarz, and A. Knopp, "SOTM measurements for the characterization of the wideband mobile satellite channel at Ku-band," in *Proc. 10th Int. ITG Conf. Syst., Commun. Coding*, 2015, pp. 1–8.
- [49] O. Kodheli et al., "Satellite communications in the new space era: A survey and future challenges," *IEEE Commun. Surveys Tuts.*, vol. 23, no. 1, pp. 70–109, Firstquarter 2021.
- [50] C.-H. Lin, C.-C. Wu, K.-F. Chen, and T.-S. Lee, "A variational autoencoder-based secure transceiver design using deep learning," in *Proc. IEEE Glob. Commun. Conf.*, 2020, pp. 1–7.
- [51] T. Lin and Y. Zhu, "Beamforming design for large-scale antenna arrays using deep learning," *IEEE Wireless Commun. Lett.*, vol. 9, no. 1, pp. 103–107, Jan. 2020.
- [52] S. Coleri, M. Ergen, A. Puri, and A. Bahai, "Channel estimation techniques based on pilot arrangement in OFDM systems," *IEEE Trans. Broadcast.*, vol. 48, no. 3, pp. 223–229, Sep. 2002.



Chia-Hung Lin (Member, IEEE) received the B.S. degree in electrical engineering from Chang Gung University, Taoyuan, Taiwan, in 2016, the M.S. degree in communication engineering from National Sun Yat-sen University, Kaohsiung, Taiwan, in 2018, and the Ph.D. degree in electrical and computer engineering from North Carolina State University, Raleigh, NC, USA, in 2023. His research interests include 6G radio, intelligent networking, machine learning and its application in wireless communications.



Shih-Chun Lin (Member, IEEE) received the Ph.D. degree from the Georgia Institute of Technology, Atlanta, GA, USA, in 2017. He is currently an Assistant Professor with the Department of Electrical and Computer Engineering, North Carolina State University, Raleigh, NC, USA, leading the Intelligent Wireless Networking (iWN) Laboratory. His research interests include 6G networks, software-defined infrastructure, machine learning techniques, mathematical optimization, and performance evaluation.



Liang C. Chu received the Ph.D. degree in electrical and computer engineering from the Georgia Institute of Technology, Atlanta, GA, USA. He is currently a Lockheed Martin Fellow with Lockheed Martin Space Systems Company (LMSSC), Lockheed Martin Corporation. He has been a Principal Investigator for many governmental and Lockheed Martin Internal Research and Development programs. He has led numerous LMSSC communications and networking systems development. Prior to joining LMSSC, he was with IBM and Bell South. He has more than 30

years of experience in communications, digital signal processing, and wireless networking. He has authored numbers of publications and holds four US patents. He was technical program committee member for IEEE Military Communications Conference.